PHYSICS AND CHEMISTRY OF SOLID STATE
V. 25, No. 4 (2024) pp. 903-909
Section: Physics

DOI: 10.15330/pcss.25.4.903-909

Vasyl Stefanyk Precarpathian National University

ФІЗИКА І ХІМІЯ ТВЕРДОГО ТІЛА
Т. 25, № 4 (2024) С. 903-909
Фізико-математичні науки

PACS: 62.23.Hj; 81.65.Cf

ISSN 1729-4428 (Print)
ISSN 2309-8589 (Online)

I.I. Skrypnyk[1], S.I. Nichkalo[1], N.O. Shtangret[2]

The effect of clustering of Si nanowires produced by the metal-assisted chemical etching method on their anti-reflecting properties

[1]*Lviv Polytechnic National University, Lviv, Ukraine, ihor.i.skrypnyk@lpnu.ua,*
[2]*Lviv State University of Life Safety, Lviv, Ukraine, shtangretnazar1993@gmail.com*

Silicon nanowires are valuable for their compatibility with silicon technology and unique properties. Using metal-assisted chemical etching, we produced silicon nanowires and studied the effects of clustering, roughness, and length on wetting. Hydrophobicity depends on silicon nanowires clustering, which is influenced by length. The highest contact angle (~95º) was for 8.5-μm long nanowires. Below 8 μm, minimal clustering promotes wetting, while longer nanowires form larger clusters and hydrophobic surfaces. The Cassie–Baxter model applies initially, transitioning to the Wenzel model over time. Adjusting surface morphology can improve anti-reflective properties. Metal-assisted chemical etching offers control over the silicon nanowires' length and wettability, benefiting silicon-based device development.

Keywords: silicon nanowires, wetting properties, super hydrophobic surfaces, metal-assisted chemical etching.

Received 03 September 2024; Accepted 15 December 2024.

Introduction

Silicon nanowires (SiNWs) have attracted substantial attention in recent years due to their compatibility with existing silicon-based technologies and their unique physicochemical properties, which open up a wide range of applications. SiNWs are considered valuable components in various fields, such as microelectronics, optoelectronics, energy harvesting, and biomedicine [1, 2]. Their remarkable surface-to-volume ratio, tunable electronic properties, and ability to be functionalized with different chemical groups make them highly versatile materials. For instance, in photovoltaics, SiNWs are used to enhance light absorption and reduce reflectivity, leading to more efficient solar cells [3-12]. Additionally, SiNWs are prominent candidates for developing superhydrophobic surfaces, which have crucial implications for self-cleaning technologies [13], anti-fouling coatings, and microfluidics [14]. Hydrophobic and superhydrophobic surfaces are of particular interest for devices that operate in moisture-prone environments or require efficient liquid handling. The ability to fine-tune the wetting properties of SiNWs by controlling their surface morphology is a critical factor in optimizing their performance in such applications. Wetting behavior, as described by the Cassie–Baxter and Wenzel models, depends on the roughness and geometric arrangement of nanostructures. Understanding the transition between these wetting regimes and how factors such as nanowire length, diameter, and clustering influence hydrophobicity remains an active area of research. Several studies have explored the use of SiNWs to create anti-reflective and hydrophobic surfaces, yet the exact role of geometric parameters in the switch between wetting states is not fully understood. In this study, we investigate the relationship between the geometric dimensions of SiNWs produced by the metal-assisted chemical etching (MACE) method and their wetting properties. By optimizing surface characteristics, the results hold potential for enhancing the performance of Si-based devices, particularly in solar energy and microfluidic applications.

I. Methods

In this section, the methods used for study the influence of the geometric dimensions of SiNWs, obtained through the MACE method, on their antireflective properties are presented. The antireflective properties, specifically the hydrophobicity, were studied using the "sessile drop" method, measuring the contact angle of the SiNWs surface of different sizes with water, further selection of experimental samples with SiNWs, measurement of their geometric dimensions and ordering. For the study, samples with SiNWs were prepared via the MACE method [15]. For this, silver particles deposited on the *n*-type Si wafers with a crystallographic orientation of (100) from a silver nitrate ($AgNO_3$) solution, followed by etching using hydrofluoric acid (HF) and hydrogen peroxide (H_2O_2).

Three samples were selected, in which the formation of nanowires was observed at different silver deposition times (15, 30, 120 sec) and different etching times (1 and 5 min.). The geometric dimensions and the spacing of the nanowires were measured using specialized software. This involved analyzing micrographs obtained with the scanning electron microscope SELMI REM106I. The measurements were carried out for all other geometric parameters, including height, diameter, and spacing. Measurements of the geometric dimensions and the arrangement period of the nanowires were conducted using the ImageJ software.

II. Results and Discussion

Figures 1–3 shows an example of measuring the distance between nanowires, and other geometric parameters such as height, diameter, and arrangement period.

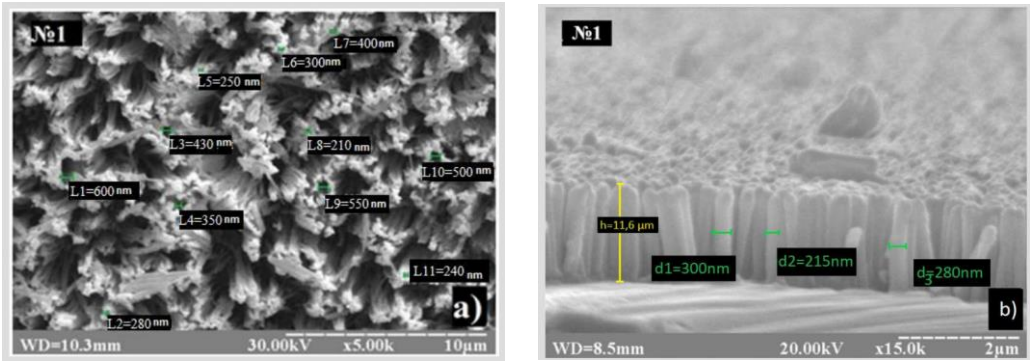

Fig. 1. SEM image of an n-type silicon wafer sample with (100) orientation after deposition of Ag particles for 15 sec and etching for 1 min: a) Top view; b) Side projection.

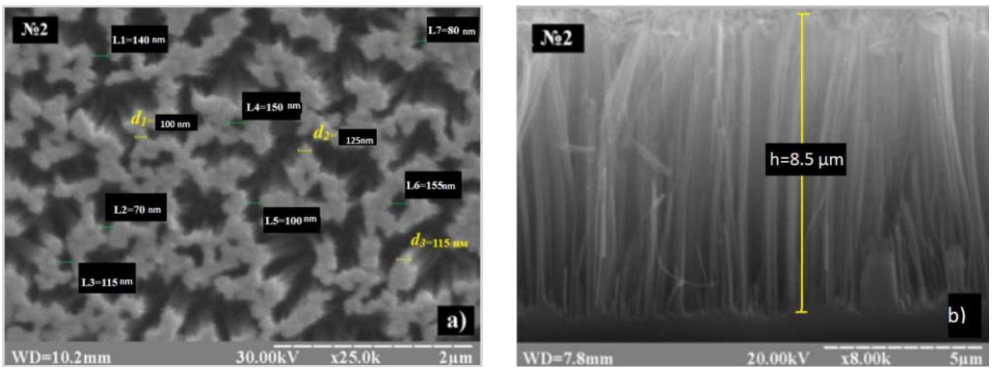

Fig. 2. SEM image of an n-type silicon wafer sample with (100) orientation after deposition of Ag particles for 30 sec and etching for 5 min. a) Top view; b) Side projection.

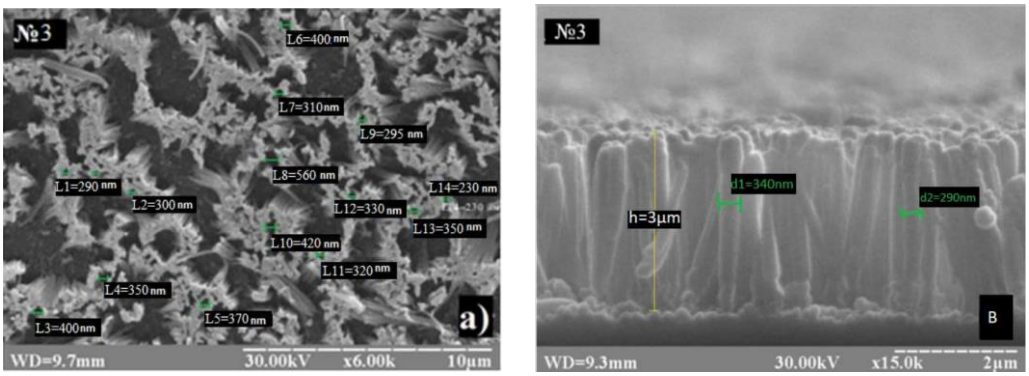

Fig. 3. SEM micrographs of an n-type silicon sample with (100) orientation after Ag deposition for 120 sec and etching for 5 min: a) top view; b) side view.

Determining the geometric parameters is important for further research. Based on the results obtained, it is possible to describe how the geometric dimensions of nanowires will affect the anti-reflective properties of the surface.

Based on the results of the studies on silicon wafers with SiNWs of various geometric dimensions and ordering on the surface, it is possible to easily determine which nanowire morphology enhances the hydrophobic properties of the surface and, accordingly, is considered the most optimal for use in microelectronic devices. Therefore, next step of the experiment was studing of the hydrophobicity of SiNWs using the "sessile drop" method. Drops of distilled water with an average volume of approximately 2 μL were applied to the surface using a syringe, and thereafter, the contact angle (θ) of water with the surface of the nanowire samples was recorded using a USB microscope. Afterward, with a 5-second interval, the contact angle was measured again. The obtained images of the contact angle of water on the surface were analyzed using the ImageJ software, which allowed for the accurate measurement of the liquid/solid interface angle. The results obtained are demonstrated in Figures 4–6.

The geometric parameters of the nanowires and the contact angles are summarized in Table 1.

As shown in Figures 4–6, the contact angle of water

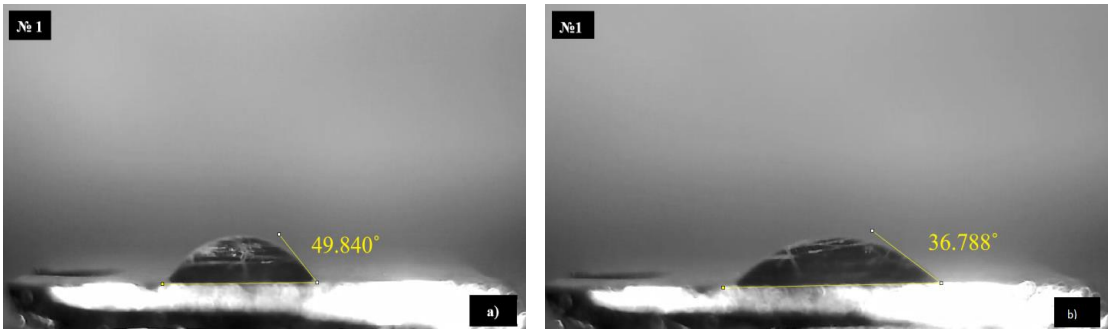

Fig. 4. Image of sample No. 1 under the microscope with a water contact angle (θ), which is: a) immediately after deposition – 49.840˚; b) after deposition with a 5-second interval – 36.788˚.

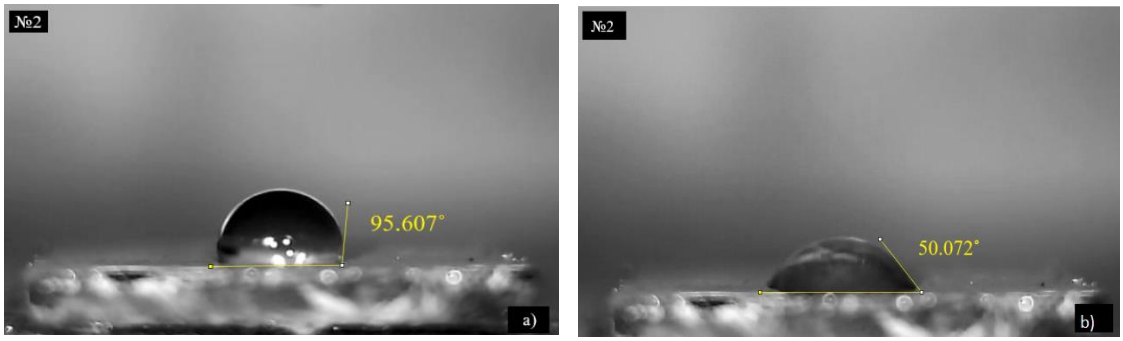

Fig. 5. Image of sample No. 2 under the Supereyes B003 microscope with a water contact angle (θ), which is: a) immediately after deposition – 95.607˚; b) after deposition with a 5-second interval – 50.072˚.

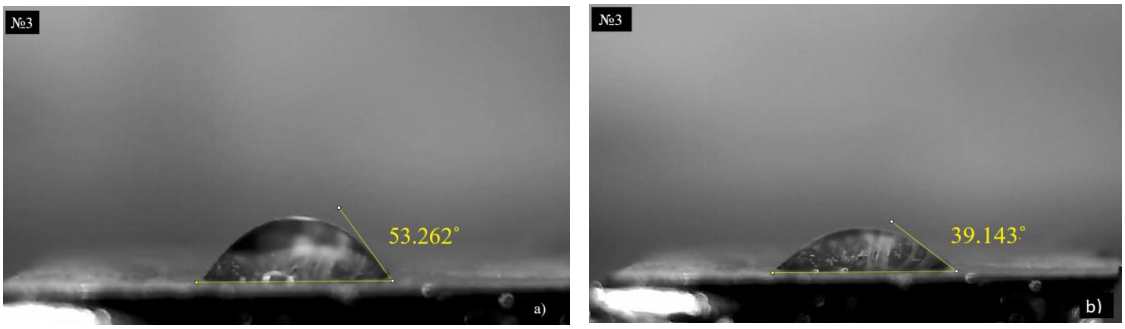

Fig. 6. Image of sample No. 3 under the Supereyes B003 microscope with a water contact angle (θ), which is: a) immediately after deposition – 53.262˚; b) after deposition with a 5-second interval – 39.143˚.

Table 1.

Geometric parameters and contact angles of silicon nanowires

№ sample	Height	Diameter	Interval	Period	Contact angle	Contact angle after 5 sec interval
1	1.6 μm	265 nm	300 nm	565 nm	49.840º	36.788º
2	8.5 μm	115 nm	115 nm	230 nm	95.607º	50.072º
3	3 μm	315 nm	350 nm	665 nm	53.262º	39.143º

decreased by approximately 25% for samples No. 1 and No. 3, and by approximately 45% for sample No. 2 after 5 seconds. The likely cause of this change is that the water droplet penetrates between the nanowires into the grooves, fully wetting the structure.

Figure 7 (a) shows the Wenzel model, which fully corresponds to the state of the silicon nanowire structure examined in this study.

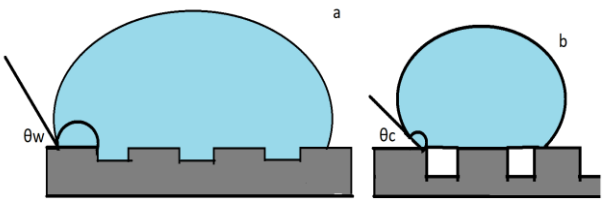

Fig. 7. Schematic representation of the homogeneous state according to the Wenzel model, where the droplet wets the surface irregularities (a), and according to the Cassie-Baxter model, where the droplet sits on the air-solid interface of the surface (b) [16].

As a result, when the rough surface beneath the droplet is completely wetted by the liquid, the equation for the apparent contact angle can be expressed as follows:

$$cos\theta = r cos\,\theta^*, \quad r = 1 + \frac{\pi dh}{(a+d)^2} \qquad (1)$$

where θ is the apparent contact angle actually measured on the surface, r is the roughness coefficient defined as the ratio of the actual surface area to its projection, and θ* is the equilibrium contact angle on an ideal smooth surface. The roughness coefficient is expressed in terms of the geometry of the supporting structures, which are silicon nanowires, as shown in Figure 8.

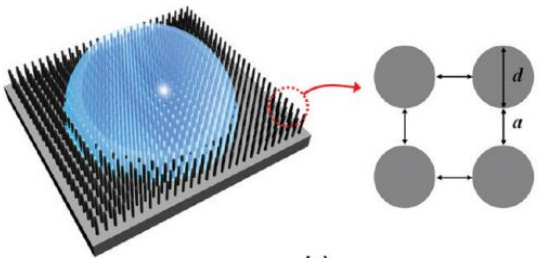

Fig. 8. Schematic diagram of a liquid droplet on the surface of a silicon substrate modified with Si nanowires [16].

However, the Cassie-Baxter model can also be applied to rough surfaces, where air is trapped within the grooves of the rough surface beneath the liquid droplet, resulting in a heterogeneous wetting regime, as shown in Figure 7 (b). The Cassie-Baxter model is generally more suitable for distinctly hydrophobic solids, while the Wenzel model applies to slightly hydrophobic surfaces ($\theta \sim 90^o$).

It is important to note how the hydrophobicity of the nanowire surface changes depending on their geometric dimensions and ordering. Figure 9 presents a graph of the measured contact angle as a function of the length of the nanowires, illustrating that the surface gradually becomes more hydrophobic as the length of the nanowires increases.

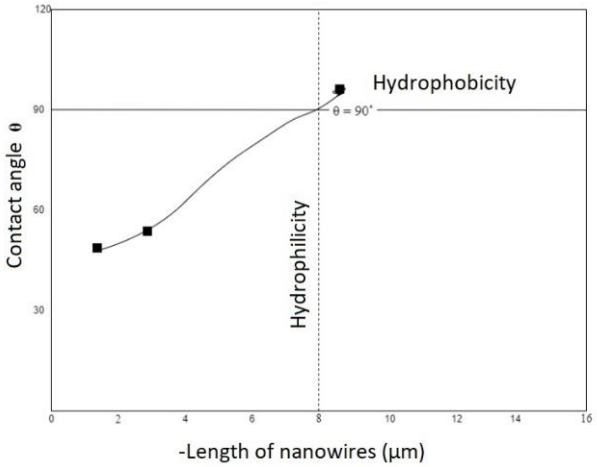

Fig. 9. Graph of the measured contact angle of water on the surface of nanowires as a function of their average length. The horizontal line at θ=90º divides the hydrophilic and hydrophobic regions. The transition from hydrophilicity to hydrophobicity of the surface occurs at a nanowire length of approximately 8 μm.

Thus, we may conclude that hydrophobicity arises at a nanowire length of approximately 8 μm and increases with longer nanowire lengths. For silicon nanowires to effectively convert solar energy, they must possess anti-reflective properties to minimize unwanted reflection losses during prolonged use. In particular, the hydrophobicity of the surface of silicon nanowires used for developing economically viable solar cells provides a self-cleaning function, which leads to the removal of accumulated dust particles from the surface of solar panels in real-world environments. It has been demonstrated that under certain conditions, the bare (i.e., deliberately uncoated or untreated) surface of silicon nanowires can exhibit hydrophobicity. The degree of hydrophobicity depends on the nature of the clustering of the nanowires, which, in turn, has been shown to depend on the length of the nanowires. It has been found that below the critical length (approximately 8 μm), clustering either does not exist or is random, thereby promoting wetting on the surface of the nanowires. As the length of the nanowires increases, the size of the clusters grows, and the surface acquires hydrophobic capability. In this case, the Cassie-Baxter model is applicable, where the droplet "sits" on the air-solid interface of the surface.

Calculation of the Equilibrium Contact Angle on an Ideal Smooth Silicon Surface Based on Obtained Results:

Input Data for Sample №1:

- Average Diameter (d): 265 nm
- Average Height (h): 1.6 μm
- Average Distance Between Nanowires (a): 300 nm
- Cosine of the Measured Contact Angle (cos θ): 0.801.

According to eq. (1), we calculate θ^* – the equilibrium contact angle on an ideal smooth surface:

$$r = 1 + \frac{3.14 \times 265 \times 1600}{(300+265)^2} = 5.17$$

$$cos\ \theta^* = \frac{cos\theta}{r} = \frac{0.801}{5.17} = 0.155$$

$$\theta^* = 81.083°$$

Input Data for Sample №2:
- Average Diameter (d): 115 nm
- Average Height (h): 8.5 μm
- Average Distance Between Nanowires (a): 115 nm
- Cosine of the Measured Contact Angle (cos θ): 0.642.

$$r = 1 + \frac{3.14 \times 115 \times 8500}{(115+115)^2} = 59.02$$

$$cos\ \theta^* = \frac{cos\theta}{r} = \frac{0.642}{59.02} = 0.0109$$

$$\theta^* = 89.276°$$

Input Data for Sample №3:
- Average Diameter (d): 315 nm
- Average Height (h): 3 μm
- Average Distance Between Nanowires (a): 350 nm
- Cosine of the Measured Contact Angle (cos θ): 0.776.

$$r = 1 + \frac{3.14 \times 315 \times 3000}{(350+315)^2} = 7.71$$

$$cos\ \theta^* = \frac{cos\theta}{r} = \frac{0.776}{7.71} = 0.1007$$

$$\theta^* = 84.221°$$

The calculated values of the equilibrium contact angle on an ideal smooth surface, determined using equation (1) for each of the samples, are summarized in Table 2.

Table 2.
Calculated values of the equilibrium contact angle on an ideal smooth surface depending on the geometric sizes of the nanowires

Sample	Height, h	Visible contact angle, θ	Equilibrium contact angle, θ^*
1	1.6 μm	36.788º	81.083º
2	8.5 μm	50.072º	89.276º
3	3 μm	39.143º	84.221º

Figure 10 shows the relationship between the visible contact angles and the equilibrium angles as a function of the length of the silicon nanowires. As we can see, the calculated equilibrium contact angles are approximately 45º lower than the measured visible contact angles. However, none of the calculated equilibrium angles reach the condition for hydrophobicity.

The obtained results indicate that the length of SiNWs is insufficient to form a hydrophobic structure. The height of the nanowires can be increased by modifying the technological conditions for producing the silicon nanowire structure, specifically by adjusting the deposition time of silver particles and the etching time.

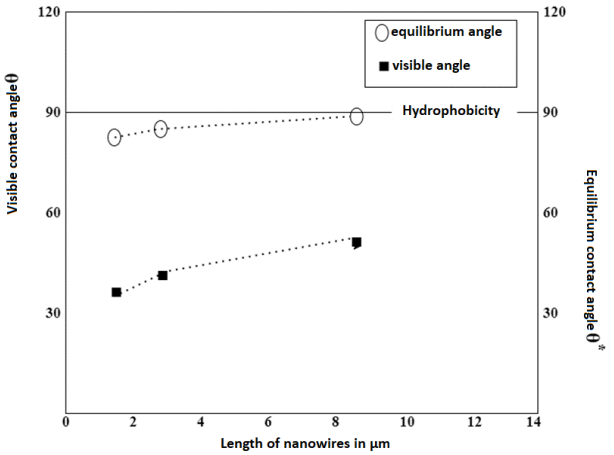

Fig. 10. Dependence of the equilibrium contact angle on an ideal smooth surface and the visible contact angle, actually measured on the surface, on the length of SiNWs.

Conclusions

For the fabrication of silicon nanowires, it is advisable to use the metal-assisted etching method, which does not require expensive and complex equipment and allows for the production of various silicon nanostructures without surface damage. The use of ImageJ software enabled accurate measurement of geometric dimensions and the arrangement period of the nanowires through the analysis of microphotographs obtained with a scanning electron microscope.

The research results on the anti-reflective properties, particularly the hydrophobicity of the silicon nanowires produced by the metal-catalytic etching method, showed that the surface hydrophobicity depends on the nature of the aggregation or clustering of the nanowires. In turn, the clustering of the nanowires depends on their length. The largest contact angle of a liquid droplet with the surface of the nanowires was obtained for samples with nanowires 8.5 μm long, which was approximately 95º. It was found that below the critical length (approximately 8 μm), there is virtually no clustering of the nanowires, or it is random, leading to surface wetting. As the length of the nanowires increases, the size of the clusters grows, and the surface acquires hydrophobic capabilities, following the Cassie-Baxter model, where the droplet "sits" on the air-solid interface. On the other hand, it was shown that after a certain period following the application of the droplet to the nanowire surface (in our case, 5 seconds), a decrease in the contact angle is observed. This may indicate that the droplet penetrates between the nanowires into the grooves, fully wetting the surface, thus implementing the Wenzel model.

The results of the calculations for the equilibrium contact angle on an ideal smooth surface showed that its maximum value is 89º. Based on the obtained results, it can be noted that the anti-reflective properties of the solid surface can be improved by altering the surface morphology. Considering the simplicity and accessibility of the metal-catalytic etching method, which allows for control over the length of Si nanowires and, as demonstrated, the degree of surface wettability, the

findings of this study may be beneficial for the development of various silicon-based devices.

Skrypnyk I.I. – Postgraduate student;
Nichkalo S.I. – Ph.D., Associate Professor;
Shtangret N.O. – Ph.D., Senior Lecturer.

[1] G. Farid, R. Amade-Rovira, Y. Ma, S. Chaitoglou, R. Ospina, E. Bertran-Serra, *Revolutionizing energy storage: Silicon nanowires (SiNWs) crafted through metal-assisted chemical etching*, Arabian Journal of Chemistry, 17, 105631 (2024); https://doi.org/10.1016/j.arabjc.2024.105631.
[2] Y. Linevych, V. Koval, M. Dusheiko, M. Lakyda, *Application of silicon nanowires in sensors of temperature, light and humidity*, Materials Science in Semiconductor Processing, 184, 108773 (2024); https://doi.org/10.1016/j.mssp.2024.108773.
[3] A.-H. Chiou, H.-Y. Liao, J.-L. Wei, *Effects of TiO_2 thin films on silicon nanowire arrays in heterojunction solar cells*, Surface and Coatings Technology, 476, 130248 (2024); https://doi.org/10.1016/j.surfcoat.2023.130248.
[4] H.-J. Li, C. Chen, X. Zhang, C. Huang, Z. Chen, T. Wang, D. Wang, L. Xu, J. Fan, *Dual-functional silicon nanowire arrays-based photocatalytic fuel cell for solar-to-electricity conversion and self-powered glucose detection*, Journal of Power Sources, 603, 234432 (2024); https://doi.org/10.1016/j.jpowsour.2024.234432.
[5] P. Nath, N. Bano, D. Sarkar, *Impact of electroplating salt ($AgNO_3$) concentration on the morphological, optical, electrical and thermoelectric properties of silver-assisted electrochemically etched silicon nanowires (SINWs)*, Current Applied Physics, 55, 53 (2023); https://doi.org/10.1016/j.cap.2023.09.002.
[6] S.P. Muduli, P. Kale, *Enhancing Si-nanowire solar cell performance through fabrication and annealing optimization*, Journal of Materials Science: Materials in Electronics, 35, 1909 (2024); https://doi.org/10.1007/s10854-024-13663-5.
[7] O. Pylypova, O. Havryliuk, S. Antonin, A. Evtukh, V. Skryshevsky, I. Ivanov, S. Shmahlii, *Influence of nanostructure geometry on light trapping in solar cells*, Applied Nanoscience, 12, 769 (2022); https://doi.org/10.1007/s13204-021-01699-6.
[8] S.F. Sajadian, M.R. Salehi, S.L. Mortazavifar, M. Shahraki, E. Abiri, *Light absorption enhancement of silicon solar cell based on horizontal nanowire arrays*, Optical Engineering, 62(3), 035109 (2023); https://doi.org/10.1117/1.OE.62.3.035109.
[9] S. Raman, R.A. Sankar, M. Sindhuja, *Advances in silicon nanowire applications in energy generation, storage, sensing, and electronics: A review*, Nanotechnology, 34, 182001 (2023); https://doi.org/10.1088/1361-6528/acb320.
[10] S. Nichkalo, A. Druzhinin, A. Evtukh, O. Bratus', O. Steblova, *Silicon nanostructures produced by modified macetch method for antireflective si surface*, Nanoscale Research Letters, 12, 106 (2017); https://doi.org/10.1186/s11671-017-1886-2.
[11] H. Hamidinezhad, A. Hayati, *VLS synthesis of silicon nanowires array for photovoltaic devices*, Silicon, 14, 10257 (2022); https://doi.org/10.1007/s12633-022-01739-y.
[12] S. Naama, T. Hadjersi, A. Larabi, G. Nezzal, *Effect of silicon wafer resistivity on morphology and wettability of silicon nanowires arrays*, Silicon, 13(3), 893 (2021); https://doi.org/10.1007/s12633-020-00511-4.
[13] R.-C. Wang, C.-Y. Chao, W.-S. Su, *Electrochemically controlled fabrication of lightly doped porous Si nanowire arrays with excellent antireflective and self-cleaning properties*, Acta Materialia, 60(5), 2097 (2012); https://doi.org/10.1016/j.actamat.2012.01.012.
[14] A. Gao., Y. Wang, T. Li, *Silicon nanowire microfluidic biosensor for multiplexed biomolecule detection*, Sensors and Materials, 30, 2693 (2018); https://doi.org/10.18494/SAM.2018.2007.
[15] S. Nichkalo, A. Druzhinin, O. Ostapiv, M. Chekaylo, *Role of Ag-catalyst morphology and molarity of $AgNO_3$ on the size control of Si nanowires produced by metal-assisted chemical etching*, Molecular Crystals and Liquid Crystals, 674(1), 69 (2018); https://doi.org/10.1080/15421406.2019.1578513.
[16] B.S. Kim, S. Shin, S.J. Shin, K.M. Kim, H.H. Cho, *Control of superhydrophilicity/superhydrophobicity using silicon nanowires via electroless etching method and fluorine carbon coatings*, Langmuir, 27, 10148 (2011); https://doi.org/10.1021/la200940j.

І.І. Скрипник[1], С.І. Нічкало[1], Н.О. Штангрет[2]

Вплив кластеризації кремнієвих нанодротів, виготовлених методом метал-асистованого хімічного травлення, на їх антивідбивні характеристики

[1]*Національний університет «Львівська політехніка», Львів, Україна, ihor.i.skrypnyk@lpnu.ua,*
[2]*Львівський державний університет безпеки життєдіяльності, Львів, Україна, shtangretnazar1993@gmail.com*

Кремнієві нанодроти цінні своїми унікальними властивостями. Використовуючи метал-каталітичне хімічне травлення, було виготовлено кремнієві нанодроти та досліджено вплив кластеризації, шорсткості та довжини на змочування. Гідрофобність залежить від кластеризації кремнієвих нанодротів, на яку впливає їх довжина. Найбільший контактний кут (~95º) був для нанодротів довжиною 8,5 мкм. Нижче за 8 мкм мінімальне утворення кластерів сприяє змочуванню, тоді як довші нанодроти утворюють більші кластери та гідрофобні поверхні. Для аналізу результатів використано модель Кессі-Бакстера з подальшим переходом до моделі Венцеля. Модифікація морфології поверхні нанодротів може покращити антивідбивні властивості. Метал-каталітичне хімічне травлення дозволяє контролювати довжину та змочуваність кремнієвих нанодротів, що може бути використано при розробці пристроїв на основі кремнію.

Ключові слова: кремнієві нанодроти, змочувальні властивості, супергідрофобні поверхні, метал-каталітичне хімічне травлення.